Available online at www.sciencedirect.com
SCIENCE DIRECT®
Organic Electronics 5 (2004) 265–270
Organic Electronics
www.elsevier.com/locate/orgel

Efficient low-molecule phosphorescent organic light-emitting diodes fabricated by wet-processing

Yuichi Hino *, Hirotake Kajii, Yutaka Ohmori

Research Center for Advanced Science and Innovation (CASI), Osaka University, 2-1 Yamada-oka, Suita, Osaka 565-0871, Japan

Received 27 February 2004; accepted 15 July 2004
Available online 8 August 2004

Abstract

We demonstrate high efficiency electrophosphorescence in organic light-emitting devices employing a phosphorescent dye doped into a low-molecule material. Methoxy-substituted 1,3,5-tris[4-(diphenylamino)phenyl]benzene (TDAPB) was selected as the host material for the phosphorescent dopant *fac*-tris(2-phenylpyridine) iridium(III) [$Ir(ppy)_3$], and organic films were fabricated by spin-coating. A peak external quantum efficiency of 8.2% (29 cd/A), luminous power efficiency of 17.3 lm/W, and luminance of 33,000 cd/m^2 were achieved at 9.4 V with a 90 nm-thick emitting layer. Emission from the host TDAPB material was not observed in the electroluminescence (EL) and photoluminescence (PL) spectra. The decrease in efficiencies at a high current is analyzed using the triplet–triplet annihilation model. The high performance for the simple device structure in this study is attributed to excellent film forming properties of the material and efficient energy transfer from the host to dopants.

Keywords: TDAPB; Starburst molecule; Phosphorescent material; Organic light-emitting diode; Simple device structure; Wet-processing

1. Introduction

Phosphorescent organic light-emitting diodes (PHOLEDs) fabricated using phosphorescent dyes have demonstrated high external quantum efficiencies [1]. Phosphorescent materials using a heavy metal containing phosphor and showing radiative emission from triplet states have been successfully used in the form of thermally evaporated small molecules [2]. To obtain high device performances, selecting a conductive host with a suitable triplet level of PHOLEDs is necessary to achieve efficient energy transfer to a dopant. Organic light-emitting diodes (OLEDs) made from small organic molecules, conjugated polymers and dendrimers as host

* Corresponding author. Tel./fax: +81 6 6879 4213.
E-mail address: hino@crcast.osaka-u.ac.jp (Y. Hino).

1566-1199/$ - see front matter
doi:10.1016/j.orgel.2004.07.001

materials have been reported earlier [3–11]. It is possible to use small organic materials to fabricate layered structures which are generally processed via evaporation. For example, a green phosphorescent dye dopant *fac*-tris(2-phenylpyridine) iridium(III) [Ir(ppy)$_3$] doped in 4,4′-*N*,*N*′-dicarbazole-biphenyl (CBP) host was reported [2]. A peak external quantum efficiency of 8.0% (28 cd/A) was obtained at 6% Ir(ppy)$_3$ doped in CBP. This result was ascribed to bipolar carrier transport in CBP along with a favorable triplet energy level alignment between the host and the dopant [12,13].

Among the small organic molecules, starburst molecules possess good hole-transport characteristics and heat resistance. OLEDs fabricated using starburst molecules for hole-transport and injection layers have demonstrated high-efficiency and long-life stability in devices [14,15]. Polymers and dendrimers can be fabricated into devices using a wet-process such as spin-coating or ink-jet printing from solution. Employing wet-processing of organic materials is useful for OLEDs fabrication, and allows for the possibility of low-cost mass production and for making large-sized screens. Poly(*n*-vinylcarbazole) (PVK) is generally used as a host material for polymer light-emitting diodes (PLEDs) because of its high triplet level for some emitting phosphorescent complexes, and it has shown high external quantum efficiencies previously [16–21]. We note that starburst molecules, which possess the superior characteristics of both small molecules and polymers such as sublimating materials and using wet-processing, would be expected to yield high-efficiency devices that can be fabricated easily.

In the present study, we have used a starburst molecule 1,3,5-tris[4-(diphenylamino)phenyl]benzene (TDAPB) as the host for the phosphorescent material Ir(ppy)$_3$ because of good hole-transport characteristics and the expectation of high triplet energy levels due to the high highest unoccupied molecular orbital (HOMO) levels. In addition, TDAPB resists crystallization due to its steric hindrance and because of its high glass-transition temperature [22]. It also possesses excellent film forming properties using wet-processing such as spin-coating. Elschner et al. reported that TDAPB was used as a buffer-layer between poly(ethylenedioxythiophene):poly(styrene sulfonic acid) (PEDOT:PSS) and the emitting layer for ITO/PEDOT:PSS/TDAPB/Alq$_3$/Mg:Ag devices [22, 23]. Compared with 2-layered (without a buffer-layer) devices, improvement in efficiencies, long-life and lowering of the electric noise were achieved in the 3-layered device. However, they referred to using a buffer-layer only because molecular phenylamine groups have been widely investigated as hole-transport materials for OLEDs.

In this work, we have used TDAPB as a host material of phosphorescent dyes and have fabricated simple devices with a hole-injection and an emitting layer.

2. Experimental procedure

Organic layers were fabricated by spin-coating onto a glass substrate coated with a patterned indium-tin-oxide (ITO) electrode. The substrate was degreased with solvents and cleaned in a UV-ozone chamber. First, a PEDOT:PSS hole-injection layer was spun over the ITO-coated glass substrate with a 35 nm-thick layer and baked in air at 120 °C for 10 min. TDAPB was used as the host for the phosphorescent material Ir(ppy)$_3$. The emitting layer which consisted of the host TDAPB, dopant Ir(ppy)$_3$ and an electron-transport material 2-(4-biphenylyl)-5-(4-*tert*-butylphenyl)-1,3,4,-oxadiazole (PBD) were dissolved in 1,2-dichloroethane. We fixed the weight ratios of the various materials TDAPB:PBD:Ir(ppy)$_3$ = 53.8%:43.0%:3.2%. This means that the content of PBD and Ir(ppy)$_3$ was 80 and 6.0 wt% for TDAPB, respectively. The TDAPB material containing Ir(ppy)$_3$ was formed by a spin-coating method separately into 90, 220 and 345 nm-thick layers. The solvent was removed by baking the samples in air at 110 °C for 10 min after spinning. The cathode, consisting of Cs/Al, was deposited in vacuum at a base pressure of $<10^{-6}$ Torr. Finally, the device was covered with a glass plate and encapsulated with epoxy resin in an argon gas atmosphere to prevent oxidation of the cathode and the organic layer. The active device area of 4 mm^2 was obtained using a shadow mask. The forward bias condition was a positive

bias with respect to the Cs/Al cathode. All measurements were carried out at room temperature in an inert gas atmosphere.

The positions of the HOMO and lowest unoccupied molecular orbital (LUMO) levels of TDAPB, PBD, and $Ir(ppy)_3$ were estimated using a low-energy photoelectron spectroscopy instrument (Rikenkeiki, AC-1). A N_2 laser with a wavelength of 335 nm was used as the excitation source. The electroluminescent (EL) spectra were measured using a photonic multichannel spectral analyzer (Hamamatsu Photonic, PMA-11). The current–voltage–luminance (I–V–L) characteristics were obtained using a 2000 multimeter (Keithley), a regulated DC power supply (Kenwood, PW36-1.5AD) and a luminance meter (Minolta, LS-100). The external quantum efficiency was calculated from the luminance, current density and EL spectrum under the assumption of the Lambertian spatial emission pattern.

3. Results and discussion

Fig. 1 shows the energy diagrams of the device showing the relative positions of the HOMO and LUMO levels of the organic layers. The TDAPB LUMO level is relatively high compared with PVK and CBP [12,15,16]. The triplet energy levels of TDAPB, however, is approximately equal to that of $Ir(ppy)_3$ (2.90 eV). Energy transfer from

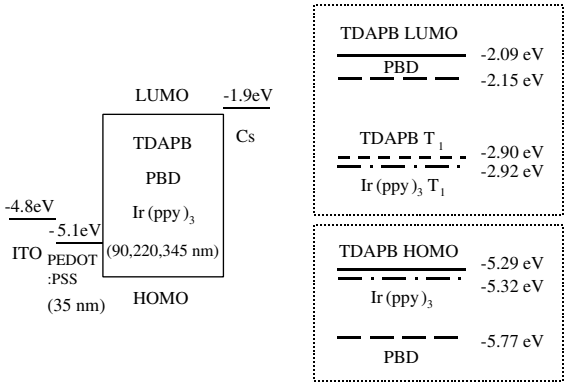

Fig. 1. Energy level diagrams of the device showing the relative positions of the HOMO and LUMO levels of the organic materials used in this study.

TDAPB to $Ir(ppy)_3$ likely occurred between the similar triplet levels of TDAPB and $Ir(ppy)_3$. The PBD LUMO level lies similar level about 0.06 eV lower to TDAPB and the HOMO level lies about 0.4 eV lower compared with that of the TDAPB and $Ir(ppy)_3$.

We tried to optimize the concentrations of $Ir(ppy)_3$ and PBD, as well as the thickness of the emission layer to obtain a higher efficiency. The optimal value of the $Ir(ppy)_3$ concentration for the external quantum efficiency was determined to be approximately 6.0 wt% for TDAPB. The devices in this study have a single layered structure, and therefore the charge balance of holes and electrons injected in the emitting layer might be influenced by carrier transport characteristics of each material. In particular, the electron-transport material PBD is indispensable to increase device performance because efficiencies and luminance both depend strongly on the concentration of PBD. At high concentrations ($\geqslant$10 wt%), the external quantum efficiency and the luminance are more than ten times as large as at low concentrations ($\leqslant$10 wt%). We optimized the doping concentration of PBD to be 80 wt% for TDAPB because of the high efficiency and considering of excellent film forming. It is effective to use PBD for the electron-transport material. TDAPB reported that is a starburst molecule functions as excellent hole-transport materials for organic EL devices [14]. At low concentrations, carriers are imbalanced in the emission layer and efficiencies decreased compared with devices at high PBD concentrations. Therefore, holes transported through the emission layer do not recombine with electrons. At high PBD concentrations, electron injection from cathode increased and the number of holes and electrons balanced in the emissive region of the device at the optimal PBD ratio for TDAPB. The optimal concentration of $Ir(ppy)_3$ is about 6.0 wt% from our study. This doping content is approximately equal to that in other OLEDs and PLEDs which have been previously reported that also used $Ir(ppy)_3$ as a dopant [2,12,13,20,21,25].

Fig. 2 shows the optical absorbance, fluorescence and phosphorescence spectra for TDAPB. Peak wavelengths for the optical absorbance, the

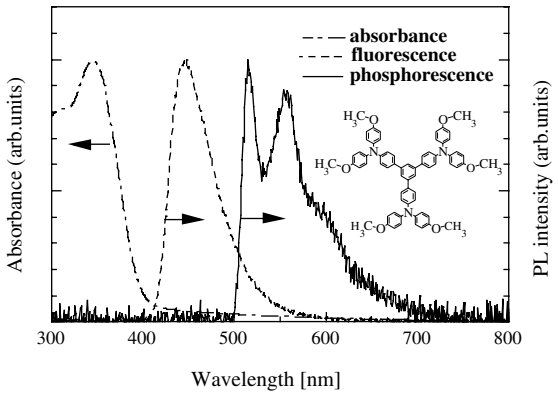

Fig. 2. Absorbance, fluorescence and phosphorescence spectra at $T = 4$ K for TDAPB. Measurements were carried out using the films which were excited with a 335 nm N_2 laser. Inset: Molecular structure of TDAPB.

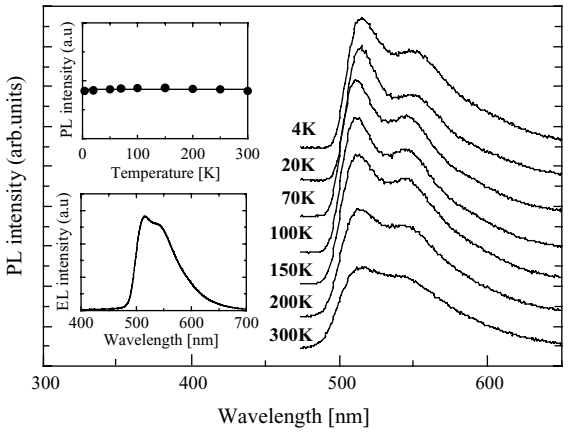

Fig. 3. Temperature dependence of the PL spectrum of a 6% $Ir(ppy)_3$ doped TDAPB film from $T = 4$–300 K. Inset: Temperature dependence of the PL intensity of the $Ir(ppy)_3$ doped TDAPB film and the EL spectrum for the 90 nm-thick device at $T = 300$ K.

fluorescence and phosphorescence are observed at 345, 440 and 518 nm, respectively. The peak of the phosphorescent spectra is approximately equal to that of PVK [24] and is expected to confine $Ir(ppy)_3$ excitons effectively. From the optical absorption and the phosphorescent spectra of TDAPB, we estimated the LUMO levels to be −2.09 eV, the triplet level to be −2.90 eV, and the HOMO levels to be −5.29 eV. The triplet energy level of host TDAPB is similar to that of the dopant $Ir(ppy)_3$ (Fig. 1).

Fig. 3 shows the temperature dependence of the PL spectra in an $Ir(ppy)_3$ doped TDAPB film from $T = 4$–300 K. The inset shows the temperature dependence of the integrated PL intensity and the EL spectrum for the 90 nm-thick layer device at $T = 300$ K. When the TDAPB film was doped with $Ir(ppy)_3$, the emission from TDAPB was quenched and an emission with a peak at 515 nm was observed. This indicates that excitation energy was successfully transferred from TDAPB to $Ir(ppy)_3$. The peak around 515 nm is hardly visible and the width of the spectra becomes broad as the temperature is increased. The PL intensity is seen to be temperature independent from $T = 4$–300 K. The EL spectrum was obtained for a current density of 0.25 mA/cm^2 and did not change under measurement. Emission was only observed from $Ir(ppy)_3$ with a peak wavelength at 515 nm, indicating efficient transfer of excitons from the TDAPB host to the dopant, and in addition, to direct formation of excitons in $Ir(ppy)_3$.

Fig. 4 shows the luminance–voltage–current density characteristics for different thicknesses of the emitting layer. The threshold voltage V_{th} was 2.5, 3.0 and 4.2 V, and the current density needed to start the emission was 0.18, 0.07 and 0.017 mA/cm^2 for 90, 220 and 345 nm thickness, respectively. The device with the 90 nm-thick layer is about ten

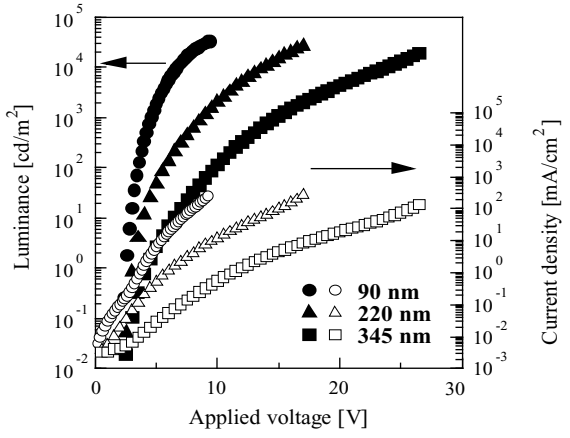

Fig. 4. Luminance–voltage–current density characteristics of ITO/PEDOT:PSS (35 nm)/TDAPB:PBD:$Ir(ppy)_3$ ((○) 90, (△) 220 and (□) 345 nm)/Cs/Al devices.

times as large in the current density when compared with that of the 345 nm-thick device. The device with the 90 nm-thick layer increased the current density because the imbalance of carriers in the emitting layer. A maximum luminance of 33,000, 27,000 and 19,000 cd/m^2 was obtained respectively for the 90, 220 and 345 nm devices.

Fig. 5 shows the dependence of the external quantum efficiency (η_{ext})–current density–power efficiency (η_p) characteristics for 6.0 wt% Ir(ppy)$_3$ doped into TDAPB for different thicknesses of the emitting layer (90, 220 and 345 nm). The solid line fits the triplet–triplet (T–T) annihilation theory. Adachi et al. analyzed T–T annihilation for Ir(ppy)$_3$ doped CBP host devices and a best fit of the model to the data were obtained [25,26]. We tried to apply the T–T annihilation theory to our devices fabricated using TDAPB as the host using the spin-coating method. All devices exhibited a gradual decrease in η_{ext} at the high current density. The external quantum efficiency η_{ext} is given by

$$\eta_{ext} = \frac{\eta_0 J_0}{4J}\left(\sqrt{1+8\frac{J}{J_0}}-1\right), \quad (1)$$

where $J_0 = 4qd/\kappa_{TT}\tau^2$, q is the electron charge, d is the thickness of the exciton formation zone, τ is the phosphorescent life time, and κ_{TT} is the T–T annihilation rate constant. The experimental data and theoretical line in Fig. 5 show a good fit at the high current density for all devices when

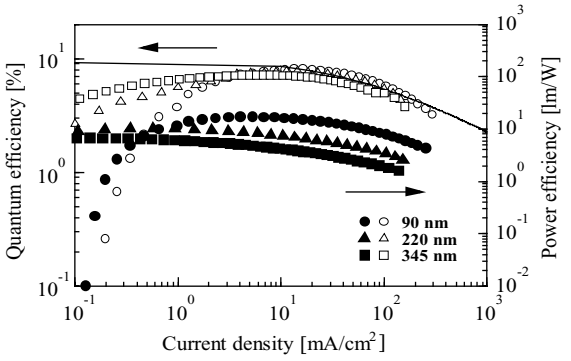

Fig. 5. External quantum efficiency (η_{ext})–current density–power efficiency (η_p) characteristics of ITO/PEDOT:PSS (35 nm)/TDAPB:PBD:Ir(ppy)$_3$ ((○) 90, (△) 220 and (□) 345 nm)/Cs/Al devices.The solid line is the triplet–triplet (T–T) annihilation model calculated using Eq. (1).

J_0 = 150 mA/cm^2. This indicates that the width of the exciton formation zone is almost the same in all devices even if the thickness of the emitting layer is changed. The maximum external quantum efficiency η_{ext} = 8.2% (corresponding current efficiency is 29 cd/A) was obtained with a 90 nm-thick layer for current density of 13.3 mA/cm^2 and luminance of 3800 cd/m^2. The power efficiency was achieved η_p = 17.3 lm/W at 4.1 mA/cm^2 and 1000 cd/m^2. The devices with 220 and 345 nm emitting layer thickness exhibited peak quantum efficiencies of 7.7% (27 cd/A) and 7.2% (24 cd/A), while the power efficiency increased with decreasing film thickness to 10.4 and 6.7 lm/W, respectively. However, the devices with a 220 and 345 nm-thick layer exhibited higher efficiencies than those with the 90 nm-thick layer at the low current ($\leqslant$1 mA/cm^2). The maximum efficiencies and luminance decreased because not only was a high threshold voltage needed to drive the devices but a decrease in the external quantum efficiency is also inferred due to the imbalance of carriers in the emitting layer with increasing thickness.

4. Conclusions

We have demonstrated improvement in the efficiency of TDAPB-based OLEDs fabricated by spin-coating. By optimizing concentrations of Ir(ppy)$_3$ and PBD, an external quantum efficiency of 8.2% and a power efficiency of 17.3 lm/W, representing the low-voltage drive, were achieved. In addition, the TDAPB device showed a high luminance, with a maximum luminance of 33,000 cd/m^2. The experimental data show a good fit to the T–T annihilation model calculations and J_0 = 150 mA/cm^2 was obtained for all devices. This means that the width of the exciton formation zone is approximately equal and not a function of the thickness of the emitting layer. Consequently, maximum efficiencies and luminance were obtained for a 90 nm-thick emitting layer. The results in this study suggest that using the starburst small-molecule TDAPB as the host of the phosphorescent material Ir(ppy)$_3$ allows for easy fabrication and is effective for achieving high efficiencies and luminance in simple device structures.

Acknowledgments

The authors thank Dr. Y. Aoki (Handai Frontier Research Center, Osaka University) for valuable discussions.

References

[1] M.A. Baldo, D.F. O'Brien, Y. You, A. Shoustikov, S. Sibley, M.E. Thompson, S.R. Forrest, Nature 395 (1998) 151.
[2] M.A. Baldo, S. Lamansky, P.E. Burrows, M.E. Thompson, S.R. Forrest, Appl. Phys. Lett. 75 (1999) 4.
[3] C.W. Tang, S.A. Van Slyke, Appl. Phys. Lett. 51 (1987) 913.
[4] J.H. Burroughes, D.D.C. Bradley, A.R. Brown, R.M. Marks, K. Mackay, R.H. Friend, P.L. Burns, A.B. Holmes, Nature 347 (1990) 539.
[5] J. Kido, K. Hongawa, K. Okuyama, K. Nagai, Appl. Phys. Lett. 64 (1994) 815.
[6] Y. Ohmori, M. Uchida, K. Muro, K. Yoshino, Jpn. J. Appl. Phys. 30 (1991) L1938.
[7] Y. Ohmori, M. Uchida, K. Muro, K. Yoshino, Jpn. J. Appl. Phys. 30 (1991) L1941.
[8] S. Tokito, M. Suzuki, F. Sato, Thin Solid Films 445 (2003) 353.
[9] S. Tokito, M. Suzuki, F. Sato, M. Kamachi, K. Shirane, Org. Electron. 4 (2003) 105.
[10] J.P.J. Markham, S.C. Lo, S.W. Magennis, P.L. Burn, I.D.W. Samuel, Appl. Phys. Lett. 80 (2002) 2645.
[11] T.D. Anthopoulos, J.P.J. Markham, E.B. Namdas, I.D.W. Samuel, S.-C. Lo, P.L. Burn, Appl. Phys. Lett. 82 (2003) 4824.
[12] M.A. Baldo, M.E. Thompson, S.R. Forrest, Nature 403 (2000) 750.
[13] C. Adachi, R. Kwong, S.R. Forrest, Org. Electron. 2 (2001) 37.
[14] Y. Shirota, Y. Kuwabara, D. Okuda, R. Okuda, H. Ogawa, H. Inada, T. Wakimoto, H. Nakada, Y. Yonemoto, S. Kawami, K. Imai, J. Lumin. 72 (1997) 985.
[15] Y. Shirota, K. Okumoto, H. Inada, Synth. Met. 111–112 (2000) 387.
[16] K.M. Vaeth, C.W. Tang, J. Appl. Phys. 92 (2002) 3447.
[17] X. Gong, J.C. Ostrowski, G.C. Bazan, D. Moses, A.J. Heeger, Appl. Phys. Lett. 81 (2002) 3711.
[18] F.-C. Chen, Y. Yang, M.E. Thompson, Appl. Phys. Lett. 80 (2002) 2308.
[19] S.-C. Chang, G. He, F.-C. Chen, T.-F. Guo, Y. Yang, Appl. Phys. Lett. 79 (2001) 2088.
[20] Y. Kawamura, S. Yanagida, S.R. Forrest, J. Appl. Phys. 92 (2002) 87.
[21] M.J. Yang, T. Tsutsui, Jpn. J. Appl. Phys. 39 (2000) L828.
[22] A. Elschner, F. Bruder, H.W. Heuer, F. Jonas, A. Karbach, S. Kirchmeyer, S. Thurm, R. Wehrmann, Synth. Met. 111–112 (2000) 139.
[23] A. Elschner, H.W. Heuer, F. Jonas, S. Kirchmeyer, R. Wehrmann, K. Wussow, Synth. Adv. Mater. 23 (2001) 1811.
[24] Y.Y. Noh, C.L. Lee, H.W. Lee, H.N. Cho, J.J. Kim, Mater. Res. Soc. Symp. Proc. 708 (2002) BB3.40.1.
[25] C. Adachi, M.A. Baldo, S.R. Forrest, S. Lamansky, M.E. Thompson, R.C. Kwong, Appl. Phys. Lett. 78 (2001) 1622.
[26] M.A. Baldo, C. Adachi, S.R. Forrest, Phys. Rev. B 62 (2000) 10967.